

The effect of foundation damage on the performance of stabilizing pillars

by M.U. OZBAY* and J.A. RYDER*

SYNOPSIS

An ERR-based methodology is presented for use in the re-assessment of the performance of stabilizing pillars, taking into account the effects of fracturing that can occur in pillar foundations under conditions of high stress. It is shown that the damage in the foundations of under-designed pillars can cause up to 30 per cent increases in ERR compared with the ERR for pillars with unfractured foundations. Despite this reduction in assessed performance, stabilizing pillars are still generally found to result in substantially lower ERR levels than alternative methods of reducing ERR, such as the use of stiff backfill or backfill ribs.

SAMEVATTING

'n ERR-gebaseerde metodologie word voorgestel vir gebruik by die herwaardering van die werkverrigting van stabiliserende pilare met inagneming van die uitwerking van breuke wat, onder toestande van hoë spanning, in pilaarfondamente voorkom. Daar word getoon dat skade aan die fondamente van onderontwerpte pilare 'n toename van tot 30 persent in die ERR kan veroorsaak vergeleke met die ERR vir pilare met ongebreekte fondamente. Ten spyte van hierdie verlagings van die geraamde werkverrigting, word daar oor die algemeen nog gevind dat stabiliserende pilare tot aansienlik laer ERR-vlakke lei as alternatiewe metodes om die ERR te verlaag, soos die gebruik van stywe terugvulling of terugvullingribbes.

Introduction

Stabilizing pillars were introduced to deep-level gold mines in the late 1960s as part of a major effort towards reducing the incidence of rockbursts on such mines¹. Their implementation was motivated from the results of theoretical studies, which indicated that the spatial rate of energy release, ERR, could be reduced by a reduction in the volumetric closure in stopes^{2,3}. In recent years, the applicability of ERR to the design of geologically disturbed, scattered mines has been called into question. Nevertheless, in deep geologically undisturbed longwall conditions, ERR has been found to continue to have both relevance and utility⁴. ERR is thus used as the prime measure of the performance of the regional support systems considered in this paper.

Experience so far has shown that, although stabilizing pillars have indeed reduced the incidence of damaging seismicity⁵, several problems have arisen as a result of their implementation. The severity of these problems (e.g. permanent loss of reef, restrictions in layout design, pillar systems themselves being potential sources of seismicity) is at present driving the mining industry to look for alternative methods of reducing the incidence of rockbursts. For example, the possibility of replacing stabilizing pillars with various types of backfill is currently being examined⁶.

Before a decision is taken as to the most efficient method of reducing ERR, it is imperative that the performance of alternative methods be determined as accurately as possible. This paper attempts to improve the methods by which the performance of stabilizing pillars (and other stiff-rib regional support systems) can be assessed.

Historically, the studies carried out on the performance of stabilizing pillars have assumed that the pillars, as well as their foundations, remain intact and behave fully elastically. However, experience shows that pillars and their foundations fracture, allowing larger volumetric closures, and thus larger ERR values, than predicted by simple elastic theory. The main object of the work described in this paper was to quantify the performance of stabilizing pillars, in terms of reducing the ERR at the mining faces, by considering the 'softening' of pillars and their foundations due to fracturing in and around the pillars. Results from modelling studies were used to give the stress-strain characteristics of pillars that softened owing to fracturing in their foundations. These characteristics were quantified in terms of 'figure of merit' parameters so that the average ERR values at faces bounded by 'soft' pillars could be determined from available analytic formulations. By the use of similar formulations, the performance of various types of backfill was also determined and compared with that of stabilizing pillars.

Method of Analysis

Although it is well known that fracturing can occur in and around pillars^{7,8}, the mechanisms involved in the fracturing process are complex and difficult to quantify. In particular, the deformations in the immediate vicinity of a deep stope tend to be inflated by large inelastic movements (bed separation, dilation of fractured rock, etc.). The approach used in this paper is therefore that 'volumetric stope closures' are estimated from far field displacements instead of from displacements that occur at the reef level. Volumetric closures so obtained are directly instrumental in generating ERR at the mining faces, whereas estimates based on actual 'skin' closures in the stopes would be greatly overstated.

* COMRO (Chamber of Mines Research Organization), P.O. Box 91230, Auckland Park, 2006 Transvaal.

© The South African Institute of Mining and Metallurgy, 1990. Paper received 15th August, 1989. SA ISSN 0038-223X/3.00 + 0.00.

To understand this method of approach, consider the three diagrams given in Fig. 1. In these diagrams, the solid lines above and below the reef show horizons prior to mining, each at a distance equal to one pillar centre-to-centre distance, $2L$. Fig. 1A assumes the strata to be intact and to behave elastically. As mining takes place in the direction perpendicular to the plane of the paper, the hangingwall and footwall move towards the mined areas, causing the horizons shown by the solid lines to move to the new positions shown by the broken lines. Because of this displacement, the gravitational potential energy drops by an amount directly proportional to the ERR at the mining faces. Fig. 1B shows a layout where pillars and their surroundings are damaged; consequently, displacements along far field horizons are larger than they are in the fully elastic system. The drop in the gravitational potential energy and thus ERR in this case is greater than those in the elastic case of Fig. 1A. Fig. 1C shows the idealized equivalent layout used in this study: the hangingwall and footwall strata are intact and behave elastically, but the pillars consist of appropriate 'soft' material that allows the far field horizons to be displaced by an amount equal to that in the inelastic system in Fig. 1B. In effect, the fractured pillar-foundation system is replaced by one comprising ribs of 'backfill' having an equivalent overall stress-strain behaviour.

The average ERR at the faces bounded by these 'soft' pillars can be determined by use of a modified version of the general analytic formula reported by Piper and Ryder⁹ for the assessment of ERR values in stopes protected by narrow backfill ribs:

$$ERR = qs_w \left(1 - \alpha + \alpha M - \frac{Lq}{\pi \lambda s_w} \ln \sin \frac{\pi \gamma}{2} \right) \dots (1)$$

In this formula, q is the vertical component of the virgin stress, s_w is the stoping width, $2L$ is the rib centre-to-centre distance, and $\lambda = E/4(1 - \nu^2)$, where E and ν are elastic modulus and Poisson's ratio, respectively. The parameter γ is the fraction of the area filled; α is called the 'lag' parameter and is defined as the ratio between the fill height and the stoping width.

For pillars, the parameter α is equal to 1, and γ relates to extraction ratio e in the form $\gamma = 1 - e$; therefore the formula given above can be re-written for soft pillar systems as

$$ERR = \frac{1}{e} \left(qs_w M - \frac{q^2 L}{\pi \lambda} \ln \sin \frac{\pi \gamma}{2} \right) \dots (2)$$

The parameter e in the denominator was introduced to account for the fact that, in a stabilizing-pillar scenario, mining is carried out over a span of $2Le$ rather than the full centres span $2L$. The parameter M in the above formulae is called 'figure of merit' and was introduced by Ryder and Wagner¹⁰ to quantify the effectiveness of backfill in reducing average face ERRs. Salamon¹¹ and Piper and Ryder⁹ showed that the figure of merit of a material can be established from an evaluation of the following simple integral of a material's stress-strain characteristics:

$$M = \frac{1}{\sigma} \int_0^{\sigma} \epsilon d\sigma \dots (3)$$

M thus represents the mean strain undergone by the material in becoming compressed to a final equilibrium stress level σ , and expresses the appropriate mathematical measure of the material's 'compressibility'. The lower the value of M , the higher the effectiveness of the backfill in reducing the ERR. In fact, when $M = 0$, equation (2) becomes

$$ERR = - \frac{q^2 L}{\pi \lambda e} \ln \sin \frac{\pi \gamma}{2} \dots (4)$$

which is identical to the average ERR at a face bounded by rigid stabilizing pillars^{9,12}.

According to equation (2), then, the determination of average ERR at a face bounded by 'soft' pillars requires establishment of the parameter M to appropriately quantify the inelastic deformations represented in Fig. 1C. The determination of M , in turn, requires the establishment of the equivalent stress-strain characteristics of the pillar and its foundations, which is discussed in the next section.

In-elastic Pillar Systems

The *in situ* measurement of stress-strain characteristics of pillar systems in deep mines is invariably a difficult task owing to the high stresses acting on the pillars and the intense fracturing around the stopes. Alternatively, the stress-strain characteristics of pillars can be obtained from numerical or physical modelling studies. However, the accuracy of the results from such studies is affected significantly, among other factors, by the boundary conditions used.

In modelling studies, the errors related to boundary conditions can be minimized by the exploitation of two important properties of elastic pillar-train layouts (Fig. 1):

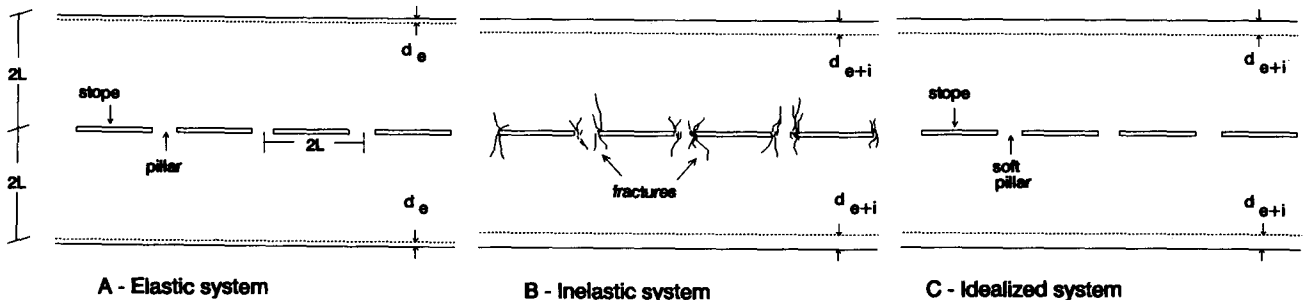


Fig. 1—Schematic diagram showing induced displacement along horizons $2L$ away from reef level in cases of elastic (A), fractured (B), and equivalent 'soft' (C) pillar systems (d_e and d_{e+i} are elastic and elastic + inelastic displacements respectively)

- (i) the stress and displacements along horizons $2L$ or more away from the reef elevation are acceptably uniform, and
- (ii) the average of displacements along *any* horizon above and below the reef is the same and equal to half of the average stope closure.

The validity of the first property is depicted graphically in Fig. 2, where stresses and displacements along the pillar and stope centrelines are plotted against distance from the reef horizon by use of the formulations given in the Addendum. The layout selected for the construction of the diagrams consists of 20 m wide pillars separated by 103 m spans, giving an extraction ratio of 85 per cent. In Fig. 2A, displacement along the pillar and stope centrelines is normalized with respect to $\pi\lambda/qL$. At the reef horizon, the displacement at the pillar centre is zero. As the distance from the reef, Z , increases, the displacement along the pillar centreline increases and becomes asymptotic to the line $\ln[1/\sin(\pi\gamma/2)]$ when $Z > 2L$. The induced displacement along the stope centreline has the value $\ln[1 + \cos(\pi\gamma/2)/\sin(\pi\gamma/2)]$ at the reef level, but also becomes asymptotic to the line $\ln[1/\sin(\pi\gamma/2)]$ when $Z > 2L$. If the pillar and stope centrelines are regarded as extremities in terms of induced displacement, it can for practical purposes be concluded that displacements along horizons $2L$ or greater away from the reef horizon are uniform. Similar conclusions clearly apply when induced stresses are under consideration.

The validity of the second property, which is predicted

by theoretical considerations, was confirmed by means of numerical modelling. In Table I, the average of the displacements calculated along horizons $4L, 2L, L, 0,5L$, as well as along the hangingwall, are given for three different extraction ratios, namely 25, 50, and 77,5 per cent. The average hangingwall sag calculated from the analytic formula given in the Addendum is also included in this table. It can be seen that, for a given extraction ratio, the average displacement along all the horizons is the same and equal to the hangingwall sag, which can be taken as half of the average stope closure. These conclusions are based on *elastic* modelling; nevertheless, it is these equivalent *elastic* closures that are instrumental in generating face ERR values. Thus, values of far field closure or volumetric closure can be used in the assessment of ERR conditions in more general, partially inelastic, environments.

Based on the properties of the pillar layout geometries discussed above, the minimum height for pillar model geometries can be established as $2L$. Also, when the symmetry conditions along the pillar and stope centrelines are considered, the geometry and boundary conditions for modelling studies can be established as shown in Fig. 3. In Fig. 3, the height and width of the model are $2L$ and L , respectively. The sides and base of the model are axes of symmetry.

Using boundary conditions similar to those mentioned above, Ozbay and Ryder¹⁴ conducted a series of numerical and physical modelling studies. In their studies,

TABLE I
AVERAGE DISPLACEMENTS (mm) ALONG VARIOUS HORIZONS IN A PILLAR LAYOUT
 $2L = 133$ m ($q = 100$ MPa)

Height of horizon	Extraction ratio = 0,25		Extraction ratio = 0,50		Extraction ratio = 0,78	
	Numerical*	Analytic†	Numerical*	Analytic†	Numerical*	Analytic†
0,0L	28,7	27,7	120,6	121,0	366,8	370,5
0,5L	28,3		120,6		366,8	
1,0L	28,4		120,6		366,9	
2,0L	28,1		120,5		367,3	
4,0L	27,3		120,5		369,7	

* By use of FLAC¹³ † By use of the analytic formula given in the Addendum

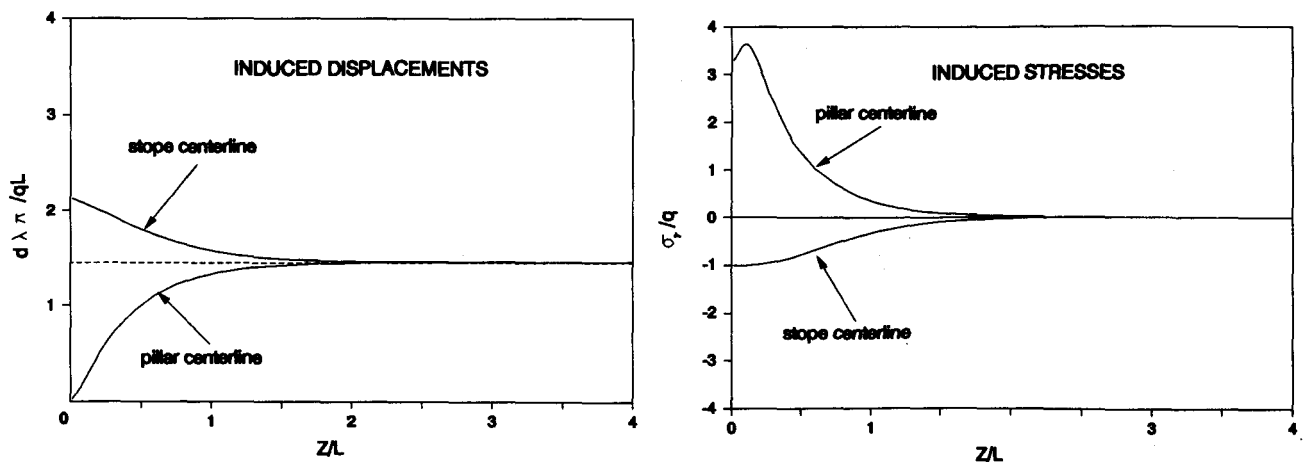


Fig. 2—Normalized induced displacement (left) and normalized induced stress (right) as functions of normalized distance from the reef horizon, Z/L .

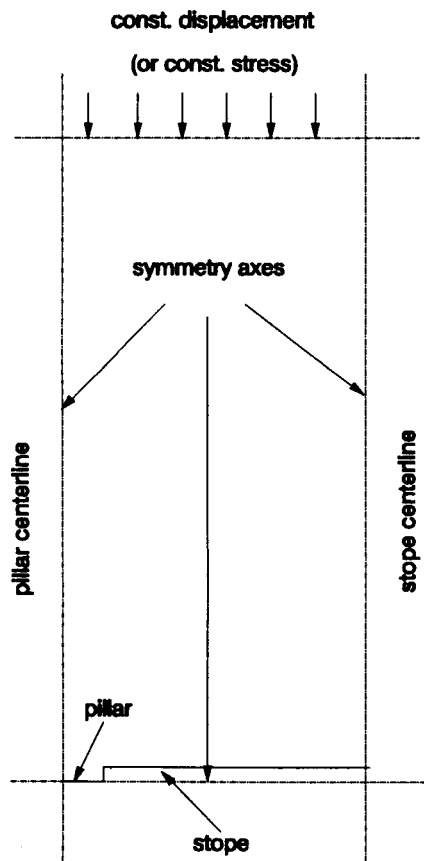


Fig. 3—Boundary conditions for the modelling of stabilizing pillars

the physical model simulated a train of pillars 28 m wide with 100 m centre-to-centre distances. Suitably confined quartzite and norite specimens were loaded up to the onset of significant fracturing in the pillar foundations. The same geometry was used for non-linear modelling using the FLAC¹³ computer program. For the numerical modelling, two sets of runs were carried out using two different failure criteria, namely the Mohr-Coulomb plastic yield and the Mohr-Coulomb strain-softening criteria. (The parameters used were $E = 93$ GPa, $\nu = 0,2$, and Mohr-Coulomb strength = $267 + 5\sigma$; and in the strain-softening modelling, the cohesion was assumed to drop linearly from 45 to 0 MPa as the plastic strain changed from 0 to 0,003.) The stress-inelastic strain relationships of pillars obtained from the numerical and physical modelling tests are summarized in Fig. 4. In this figure, the elastic strains that occurred while the pillars and their foundations were intact are excluded to account for the deformation increases due only to fracturing in and around the pillars.

Fig. 4 shows that the strain-softening and Mohr-Coulomb plastic models result in the largest and smallest inelastic closures, respectively. The inelastic strains in the physical model tests lie between the two numerical modelling curves. At present, available knowledge of the behaviour of large-scale *in situ* pillars is insufficient to prove or disprove any of the stress-strain relationships given in Fig. 4. In the evaluation of the performance of stabilizing pillars in the next section, however, the curve obtained from the numerical modelling based on the strain-softening failure criterion (worst case) is assumed

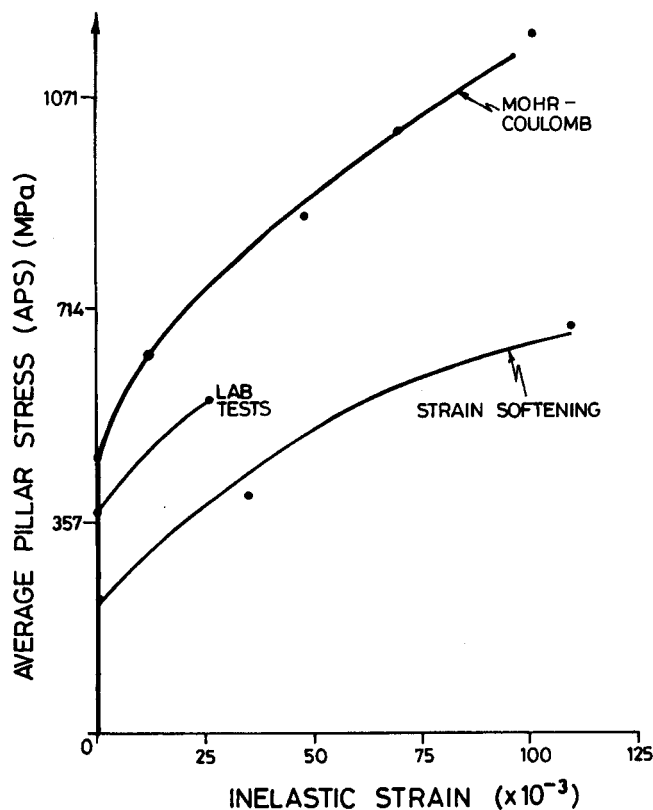


Fig. 4—Stress-inelastic strain characteristics of squat pillar systems as obtained from numerical and physical modelling studies

to represent the stress-strain relationships of pillars with damaged foundations.

Behaviour of Stabilizing Pillars

On the assumption that the stress-strain characteristic given by the strain-softening modelling describes the behaviour of stabilizing pillars, the figure of merit M for these pillars can be calculated from the application of equation (3) to the 'strain-softening' curve given in Fig. 4. It is important to note that, in equation (3), the upper bound of the integral is defined by the average pillar stress, APS. Thus the value of M depends on the mining depth and extraction ratio ($APS = q/(1 - e)$). For example, for an extraction of 85 per cent at a depth of 3000 m, the average stress acting on pillars is 540 MPa. When the integration in equation (3) is done within the bounds of 0 and 540, the value for M is determined as 0,04. The value of M for the same layout but at a depth of 4000 m is 0,07 since APS at this depth is 720 MPa.

Once the figure-of-merit value has been established for a particular pillar layout, the average ERR at the faces bounded by the pillars can be calculated from equation (2). In Fig. 5, average ERR is plotted as a function of M in terms of equation (2) for two different mining depths and extraction ratios, with $2L = 133$ m and the stoping width = 1 m in all cases. The broken horizontal line shows a maximum acceptable ERR level of 30 MJ/m². The vertical axes represent $M = 0$; therefore the ERR values for unfractured pillars can be read directly from these axes. For example, when $H = 4000$ m, $e = 0,85$, and $M = 0$, the ERR at the face bounded by 20 m

wide intact pillars can be found from Fig. 5—or equation (4)—to be 23 MJ/m². If these pillars and their foundations are fractured and their behaviour is taken to be similar to that defined by the 'strain-softening' plot in Fig. 4, the calculated ERR rises to 32 MJ/m² based on the *M* value of 0,07 established above.

For the particular case discussed above, fracturing in and around pillars can cause a roughly 30 per cent increase in ERR compared with that for intact pillars. Despite this increase, the ERR is still close to the limiting ERR level of 30 MJ/m². At shallower depths (*H* < 4000 m) or with smaller extraction ratios (*e* < 0,85), the ERR values in pillar layouts remain below 30 MJ/m².

To make the performance evaluation of stabilizing pillars more meaningful, the stress-strain characteristics of pillar systems are compared with those of typical fill materials in Fig. 6. In this figure, the behaviour of stabilizing pillars is assumed to be defined by the curve marked as 'strain-softening' in Fig. 4. The backfill behaviour is assumed to be governed by the hyperbolic equation (representative for a 'good'-quality full-plant tailings backfill material⁹):

$$\sigma = \frac{5\epsilon}{0,3 - \epsilon}, \dots\dots\dots (5)$$

where σ is the stress in megapascals (MPa) acting on the fill and ϵ is the fill strain. The stress-strain relationship for a higher-quality fill—a 20 per cent cemented, crushed-waste material—is assumed to be governed by an initial modulus¹⁵ of 1600 MPa and the following hyperbolic equation:

$$\sigma = \frac{1600 \times 0,3\epsilon}{0,3 - \epsilon} \dots\dots\dots (6)$$

The plots given in Fig. 6 can be used, with equation (3), to obtain *M* values for these types of backfill for a given final average stress level. Table II gives *M* values for various average stresses acting on stabilizing pillars and backfill systems. As seen in this table, the *M* values for tailings backfill are less sensitive to changes in applied stress levels, but are numerically much larger than the *M* values associated with stabilizing pillars or cemented waste. For the same average stress level, if the effects of

possible foundation failure are ignored, cemented waste ribs result in smaller *M* values than tailings backfill, but substantially larger *M* values than stabilizing pillars. Stabilizing pillars are therefore expected to perform much more effectively in reducing ERR than the backfill types considered under the same average stress levels.

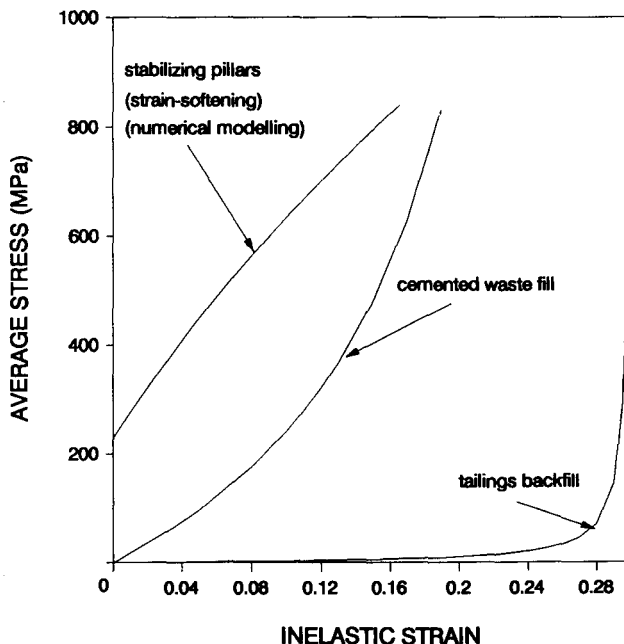


Fig. 6—Stress-inelastic strain characteristics in stabilizing pillar systems, and two types of backfill in confined compression

The average stress for cemented-waste ribs can be reduced by an increase in the amount of placement in the stopes. For example, at a given depth, if the amount of placement is increased from 15 to 30 per cent, the average stresses on the ribs are halved. According to Table II, the *M* values for cemented-waste ribs with 30 per cent placement are still slightly greater than those for 85 per cent extracted pillar layouts. Furthermore, unless special attention is given to reducing the 'lag' parameter α in equation (1), the ERR associated with a 30 per cent placed cemented-waste layout is expected to be substantially

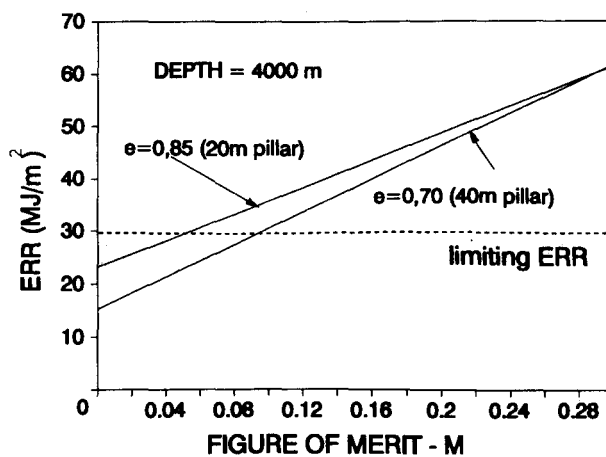
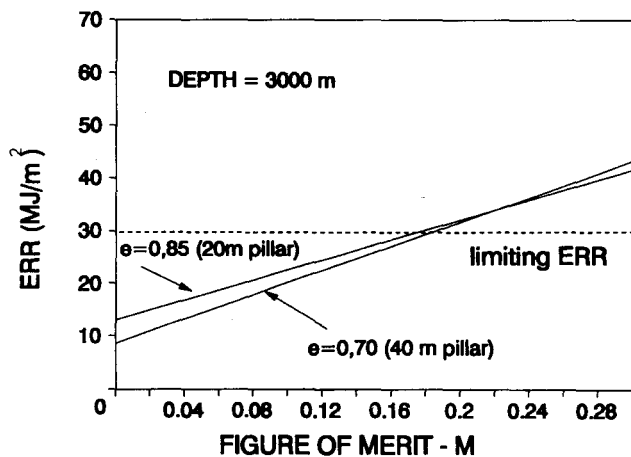


Fig. 5—Energy release rate (ERR) as a function of figure of merit (*M*) for various extraction ratios (*e*) in stabilizing pillar layouts when $2L = 133$ m

TABLE II

FIGURE-OF-MERIT VALUES FOR SQUAT STABILIZING PILLARS, AND CEMENTED-WASTE AND TAILINGS BACKFILL AT VARIOUS AVERAGE STRESS LEVELS

Average stress MPa	Stabilizing pillar (with damaged foundations)	Cemented waste (with foundation damage)	Tailings backfill
81	0,00	0,02	0,25
135	0,00	0,04	0,26
180	0,00	0,05	0,27
270	0,00	0,06	0,27
360	0,01	0,08	0,28
540	0,04	0,10	0,29
720	0,07	0,12	0,29

larger than the ERR resulting from an 85 per cent extracted pillar layout.

As a further illustration of the effect of foundation damage, and of figure-of-merit and lag parameters, on ERR, consider a stabilizing-pillar layout at a depth of 4000 m with an extraction ratio of 85 per cent and $2L = 133$ m. In this case, as already stated, $APS = 720$ MPa, $M = 0,07$, and $ERR = 32$ MJ/m².

The use of 30 per cent cemented waste placed in advanced headings will result in $APS = 360$, $M = 0,08$, and $\alpha = 0,95$. In this case, the ERR can be calculated from equation (2) modified to account for the faces mined between the cemented waste ribs, that is

$$ERR = \frac{qs_w}{(1 - \gamma)} \left(1 - \alpha + \alpha M - \frac{Lq}{\pi \lambda s_w} \ln \sin \frac{\pi \gamma}{2} \right), \quad (8)$$

which gives $ERR = 35$ MJ/m². Alternatively, the use of 30 per cent normally placed tailings-backfill ribs will result in $APS = 360$ MPa, $M = 0,28$, $\alpha = 0,75$ and, according to equation (1), $ERR = 60$ MJ/m². If 100 per cent tailings backfill is placed, ERR can be calculated to be 47 MJ/m² from the formula^{11,9}:

$$ERR = qs_w(-\alpha + \alpha M). \dots\dots\dots (9)$$

The layouts and fill materials discussed above are thought to be approximations of a number of practical cases and, as the results show, among the cases considered, the lowest face ERR values continue to be provided by the stabilizing pillars, even when the damage that occurs in their foundations is taken into account. The use of very stiff fill materials, such as pre-placed wide concrete ribs having initial moduli higher than 10 GPa⁶, could modify this conclusion, which should not be taken to be general. Such scenarios are currently being investigated by the general methodology presented above¹⁵.

Summary

The paper shows that damage caused in and around stabilizing pillars by fracturing under high stresses can reduce their effectiveness. For example, at a depth of 4000 m, a damaged pillar system can conservatively give rise to 30 per cent greater ERRs than an unfractured pillar system. Despite this reduction in performance, stabilizing pillars appear to provide at least as effective a method of reducing ERR as the alternative methods considered

here, such as the use of cemented crushed-waste ribs or tailings backfill.

It should be noted that the analyses carried out in this paper were based on the stress-strain characteristics of stabilizing pillars obtained solely from studies employing numerical and physical modelling. By use of the methodology introduced in this paper, more realistic evaluation of the performance of stabilizing pillars or stiff-fill rib systems can be achieved if their *in situ* stress-strain characteristics are included as soon as these become available.

Addendum

The theoretical analyses are based on a general analytic solution given by Salamon¹² for an infinite train of pillars with a centre-to-centre spacing of $2L$ and a pillar width of $2a_p$.

$$\begin{aligned} \gamma &= \frac{\alpha_p}{L} \\ ch &= \cosh\left(\frac{\pi Z}{2L}\right) \\ sh &= \sinh\left(\frac{\pi Z}{2L}\right) \\ c &= \cos\left(\frac{\pi \gamma}{2}\right) \\ s &= \sin\left(\frac{\pi \gamma}{2}\right), \end{aligned}$$

and taking the origin of the complex coordinate system $\omega = x + iZ$ at the centreline of the stope, Salamon's complex potential takes on the form

$$\psi(\omega) = \omega - L + \frac{2L}{\pi} \arg \sin \left(\frac{\cos(\pi\omega/2L)}{s} \right).$$

Evaluation of the real and imaginary parts of this function and its derivatives at hangingwall points along the stope centreline (i.e. at $\omega = 0 - iZ$) and along the pillar centreline (i.e. at $\omega = L - iZ$), and substitution into Salamon's expressions for vertical induced stress σ_z and displacement d , the following results are obtained:

$$\begin{aligned} \left(\frac{\sigma_z}{q}\right)_{stope-c/l} &= -1 + \frac{sh}{\sqrt{sh^2 + c^2}} - \frac{\pi Z}{2L} c^2 \frac{ch}{(sh^2 + c^2)^{3/2}} \\ \left(\frac{\sigma_z}{q}\right)_{pillar-c/l} &= -1 + \frac{ch}{\sqrt{sh^2 + s^2}} + \frac{\pi Z}{2L} c^2 \frac{ch}{(sh^2 + s^2)^{3/2}} \\ \left(\frac{\pi \lambda}{qL}\right) d_{stope-c/l} &= \operatorname{argcosh}\left(\frac{ch}{s}\right) - \frac{\pi}{4(1-\nu)L} \left(1 - 2\nu + \frac{sh}{\sqrt{sh^2 + c^2}}\right) Z \end{aligned}$$

$$\left(\frac{\pi\lambda}{qL}\right) d_{pillar-c/l} = \operatorname{argsinh}\left(\frac{sh}{s}\right) - \frac{\pi}{4(1-\nu)L} \left(1 - 2\nu + \frac{sh}{\sqrt{sh^2 + s^2}}\right) Z$$

The mean hangingwall closure, s_h , averaged over the full span $2L$ can be found when half of the volumetric closure of a stope is divided¹⁶ by $2L$, the result being

$$s_h = \frac{qL}{\pi\lambda} \ln\left(\frac{1}{s}\right).$$

Acknowledgement

The work described in this paper is part of the research programme carried out at COMRO (Chamber of Mines Research Organization). Permission to publish the results is gratefully acknowledged.

References

1. ORTLEPP, W.D., and SPOTTISWOODE, S.M. The design and introduction of stabilizing pillars at Blyvooruitzicht Gold Mining Company Limited. *Proceedings 12th CMMI Congress*. Glen, H.W. (ed.). Johannesburg, South African Institute of Mining and Metallurgy, 1982. pp. 353-363.
2. COOK, N.G.W., and SALAMON, M.D.G. The use of pillars for stope support. Johannesburg, Chamber of Mines of South Africa, unpublished report, 1966.
3. SALAMON, M.D.G. Elastic analysis of displacements and stresses induced by the mining of reef deposits. *Symposium on Rock Mechanics and Strata Control in Mines*. Johannesburg, South African Institute of Mining and Metallurgy, 1965. pp. 71-92.
4. ANON. *An industry guide to methods of ameliorating the hazards of rockfalls and rockbursts*. Johannesburg, Research Organization, Chamber of Mines of South Africa, 1988. pp. 84-94.

5. GURTUNCA, R.G., JAGER, A.J., ADAMS, D.J., and GONLAG, M. In situ measurements of backfills and surrounding rockmass behaviour in South African gold mines. *Proceedings 4th International Symposium on Mining with Backfill*, Ontario, Canada, October 1989.
6. ADAMS, D.J., GURTUNCA, R.G., JAGER, A.J., and GAY, N.C. Assessment of a new mine layout incorporating concrete pillars as regional support. *Ibid.*
7. BRUMMER, R.K. Fracturing and deformation at the edges of tabular gold mining excavations and development of a numerical model describing such phenomena. Johannesburg, Rand Afrikaans University, Ph.D. thesis, 1987.
8. HAGAN, T.O. An evaluation of systematic stabilizing pillars as a method of reducing the seismic hazard in deep and ultra-deep mines. Johannesburg, University of the Witwatersrand, Ph.D. thesis, 1987.
9. PIPER, P.S., and RYDER, J.A. An assessment of backfill for regional support in deep mines. *Backfill in South African mines*. Johannesburg, South African Institute of Mining and Metallurgy, 1988. pp. 111-136.
10. RYDER, J.A., and WAGNER, H. 2D analysis of backfill as a means of reducing ERR at depth. Johannesburg, Chamber of Mines of South Africa, unpublished report, 1978.
11. SALAMON, M.D.G. Rockburst hazard and the fight for its alleviation in South African gold mines. *Rockbursts: Prediction and control*. London, Institution of Mining and Metallurgy, 1983. pp. 11-36.
12. SALAMON, M.D.G. Two-dimensional treatment of problems arising from mining of tabular deposits in isotropic or transversely isotropic ground. *Int. J. Rock Mech. Min. Sci.*, vol. 5, 1963. pp. 159-185.
13. CUNDALL, P.A. FLAC user's manual, version 2.01, 1987.
14. OZBAY, M.U., and RYDER, J.A. (1989). Investigations into Foundation Failure Mechanism of Hard-Rock squat rib pillars. Rock at Great Depth, Int. Symp. ISRM-SPE, Pau, France.
15. GURTUNCA, R.G. Personal communication, 1989.
16. RYDER, J.A. Rational function analysis of tabular excavations in two dimensions. Johannesburg, Chamber of Mines of South Africa, unpublished report, 1984.

Publications from Chapman & Hall

The following publications can be ordered at the prices quoted from Alison West, Promotion Department, Chapman & Hall, New Fetter Lane, London EC4P 4AB, England.

● *Handbook of metal treatments and testing*, by R.B. Ross. 2nd ed. 1988, 590 pp. \$35.00.

This handbook has been thoroughly updated for this new edition and re-organized for easier access to the information. The aim is to list and describe every process known by the author that can be applied to the use and treatment or testing of metals. The book is designed to be used by practising engineers.

● *Introduction to corrosion and protection of metals*, by G. Wranglen. 2nd ed. 1985, 272 pp., hardback: £34.00, paperback: £15.95.

● *Materials science*, by J.C. Anderson, K.D. Leaver, R.D. Rawlins, and J.M. Alexander. 4th ed. 1989,

576 pp., £17.95.

● *Journal of Materials Science and Journal of Materials Science Letters*, edited by W. Bonfield. 1989 subscription: £785.

The *Journal of Materials Science* and its companion journal, the *Journal of Materials Science Letters*, are leading primary and short communications journals in the field, reaching an international audience. They publish consistently high-quality work from around the world and are of use to all researchers in materials science. The Journals contribute to the development of materials science research through an international and interdisciplinary approach. To this end the journals are broadly based, covering the structures and properties of all engineering materials with a growing emphasis on materials used in the rapidly expanding information-handling micro-technology field.